

Dielectric Property Change From Perovskite Type Oxide Films with Multi-Layered Structures

Takatoshi.Matsuo¹, Takashi.Teranishi¹, Takakiyo.Harigai¹, Song-Min.Nam^{1, 2}, Hirofumi.Kakemoto¹, Satoshi.Wada¹ and Takaaki.Tsurumi¹

¹Tokyo Inst. of Tech, 2-12-1 Ookayama, Meguro-ku, Tokyo 152-8550, Japan

Fax: 81-03-5734-2514, e-mail: matsuo@cim.ceram.titech.ac.jp

²National Institute of Advanced Industrial Science and Technology (AIST), AIST Tsukuba East, Tsukuba, Ibaraki 305-8564, Japan

BaTiO₃/SrTiO₃ (BTO/STO) multi-layered films on MgO(100) substrates were fabricated by RF sputtering method. BaTiO₃ and SrTiO₃ were alternately deposited using two ceramic targets. A solid solution film with a chemical composition of (Ba_{0.5}Sr_{0.5})TiO₃ was also prepared. X-ray pole figures indicated that the films had an epitaxial relation with the substrate. Planer electrodes were formed on the films using a lithography technique. The complex admittance of the thin film was measured with an impedance analyzer from 1 MHz to 3 GHz. Dielectric permittivity of the films was determined from admittance data using an electromagnetic field analysis. The film of [(BaTiO₃)₁₀/(SrTiO₃)₁₀]₅₀ showed a high dielectric constant up to 850 in comparison with the solid solution film that of 200.

Key words: BaTiO₃, SrTiO₃, multi-layered film, RF-sputtering, dielectric constant, microwave

1. Introduction

Artificial super-lattices of oxide materials are of interest in numerous applications as electric devices because the super-lattices have the potential to drastically improve material properties and the bulk materials with the perovskite-type structure exhibit various properties so that the artificial superlattices, in which materials with different properties are stratified at an atomic level, are expected to be one of the most interesting systems in the research of the oxide superlattices.

Some research groups have succeeded in fabricating artificial super-lattices of the perovskite BTO/STO, and their superlattices show different behaviors from solid solutions between BTO and STO[1,2,3]. In the our previous study, dielectric properties of several kinds of BTO/STO superlattices were measured, and it was reported that dielectric constants of the BTO/STO artificial superlattices on STO(100) substrates by the molecular beam epitaxy (MBE) process showed giant dielectric constants (Fig. 1). Particularly,

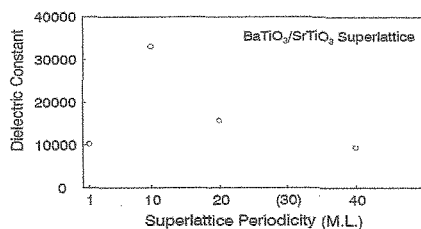


Fig. 1. Dielectric constant of BTO/STO superlattices measured at 110MHz as a function of periodicity of superlattices.

BTO/STO superlattices with a periodicity of 10 units cells of the perovskite structure showed a maximum dielectric constants of over 30,000

Therefore this material has versatile applications, for example, tunable capacitor, high frequency devices and so on. However, all this time artificial super-lattices were fabricated by the MBE method. The MBE method could control atomic layer epitaxy growth, but the growth speed is extremely slow, and only small quantity was obtained at a time. Therefore the MBE process is not suitable for industrial production process. To solve those problems, we tried to fabricate BTO/STO multi-layered films on MgO (100) substrate by RF magnetron sputtering method.

In this paper, we reported the dielectric constant of BTO/STO multi-layered films that were fabricated on MgO (100) substrate by RF magnetron sputtering method. After, the structure of the multi-layered films were represented by a formula [(BTO)_m/(STO)_m]_n, where the subscript m indicates the period of layers ($m=10$ and 50) and n indicates the number of lamination layer ($n=50$ and 10).

2. Experimental

2.1 Sample preparation

BTO/STO multi-layered films and (Ba_{0.5}Sr_{0.5})TiO₃ (BST) solid solution films were deposited on STO thin films which was deposited on MgO(100) substrates using RF sputtering

Table I. Sputtering condition of all films.

	STO	BST	Multi-layered BTO	Multi-layered STO
Deposition on	MgO substrate	STO film	Multi-layered STO film	Multi-layered BTO film
Target	SrTiO ₃	Ba _{0.5} Sr _{0.5} TiO ₃	BaTiO ₃	SrTiO ₃
Deposition temperature	750°C	650°C	600°C	600°C
Gass pressure	50 mTorr	50 mTorr	50 mTorr	50 mTorr
Gass composition	Ar:O ₂ = 4:1	Ar:O ₂ = 4:1	Ar:O ₂ = 4:1	Ar:O ₂ = 4:1
RF power	30 W	80 W	120 W	30 W

method. The Ar and O₂ mixed gas was used for sputtering. Its composition was Ar:O₂=4:1. And total pressure was 50 mTorr at film preparation. BTO and STO were alternately deposited using those of ceramic targets. The diameter of the targets was 33 mm. And the targets were 80 mm oppositely away from the MgO(100) substrate. At first, STO film was fabricated on MgO(100) substrate, the substrate temperature (T_{sub}) and RF power (P_{RF}) were set at 750°C and 30 W, respectively. BST film was then fabricated on STO/MgO(100). The T_{sub} and P_{RF} were kept at 650°C and 80 W. BTO/STO multi-layered film was also fabricated on STO/MgO(100). The T_{sub} and P_{RF} were 600°C, 120 W(BTO) and 30 W(STO). All conditions were listed in Table I.

2.2 Characterization of films

The crystallinity, crystallographic orientation, film thickness, and microstructure were characterized using x-ray diffraction (XRD, θ -2 θ scan), x-ray pole figure, and scanning electron microscope (SEM).

Micro-sized planner electrode was fabricated by electric beam lithography followed by lift-off method after Au-sputtering. The complex admittances of a formed electrode were measured from 1 MHz to 3 GHz with an impedance analyzer (Agilent Technology, E4199A). Before the measurement of the samples, the calibration was performed by open, short and load state using an impedance standard substrate kits (Cascade Microtech). The high-frequency planner analysis was carried out using commercial software (Sonnet-em) to calculate the design the electrode pattern suitable for the measurement of the samples.

3. Results and Discussion

3.1 Determination of deposition rate

Firstly, to control the thickness of multi-layered films, the growth rate of each layer should be evaluated. To define the each layer's deposition rate, three kinds of samples were prepared. 1) STO film on MgO(100) substrate was prepared with 7200 sec deposited time (Sample 1). 2) BTO film on STO/MgO(100) (Sample 1) with 7200 sec deposited time (Sample 2). 3) STO film on BTO/STO/MgO(100) (Sample 2) with 7200 sec deposited time (Sample 3).

To measure the thickness of films, cross-sectional SEM photograph was taken about

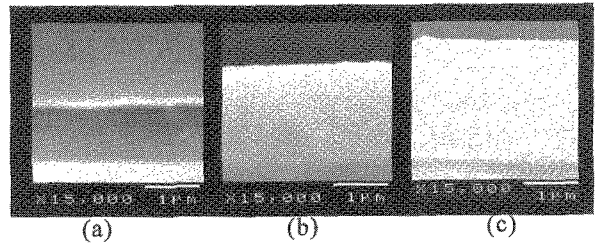


Fig. 2. Cross sectional SEM (a) sample1 (STO/MgO), (b) sample 2 (BTO/STO/MgO) and (c) sample 3 (STO/BTO/STO/MgO).

all samples (Fig. 2). From Fig. 2(a), (b) and (c), the boundary of STO and multi-layered BTO can be seen. This showed that growth rate was not change almost constantly. From this cross-section SEM photograph for Sample1 in Fig. 2(a), the growth rate of STO/MgO (100) substrate was estimated to be 10 nm/min. Sample 1 and 2 in Fig. 2(a) and (b), the growth rate of multi-layered BTO film on STO/MgO (100) substrate was also estimated to be 7.0 nm/min. Sample 3 and Sample 2 in Fig. 2(b) and (c), the growth rate of STO multi-layered film was estimated to be 3.4 nm/min. Each layer's growth rate was listed in Table II.

Table II. The thickness of each layer.

Layer	Growth rate (nm/min)
STO film on MgO substrate (STO/MgO)	10.0
BTO film on STO/MgO (BTO/STO/MgO)	7.0
STO film on BTO/STO/MgO	3.4

Based on this growth rate (Table II.), we prepared four samples. 1) [(BTO)₁₀/(STO)₁₀]₅₀ multi-layered film on STO/MgO (BT/ST50). 2) [(BTO)₅₀/(STO)₅₀]₁₀ multi-layered film on STO/MgO (BT/ST10). 3) BST film on STO/MgO (BSTS). 4) STO film on MgO (ST). The thickness of multi-layered film was designed 400 nm and total thickness of BT/ST50 and BT/ST10 were designed 800 nm. All samples information and each layer's deposition time were shown in Fig. 3.

3.2 Crystallinity and orientation of samples

All films were characterized by XRD and x-ray pole figure to be single phase and exclusively *c*-axis oriented epitaxial growth (Fig. 4). However satellite peaks based on a super lattice structure was not observed. This showed that BT/ST50 and BT/ST10 didn't have an artificial super-lattices structure.

Cross sectional SEM photographs of all samples was shown in Fig. 5. From Fig. 5, each sample's thickness was determined. The thickness of the BT/ST50 and BT/ST10 were thinner than the estimated thickness. It

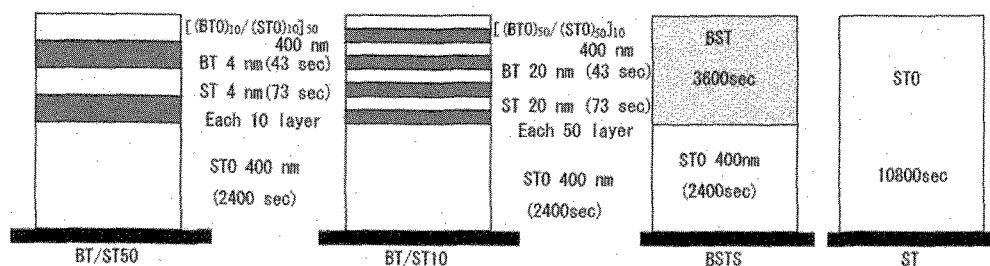


Fig. 3. Prepared samples information and deposition time of each layer.

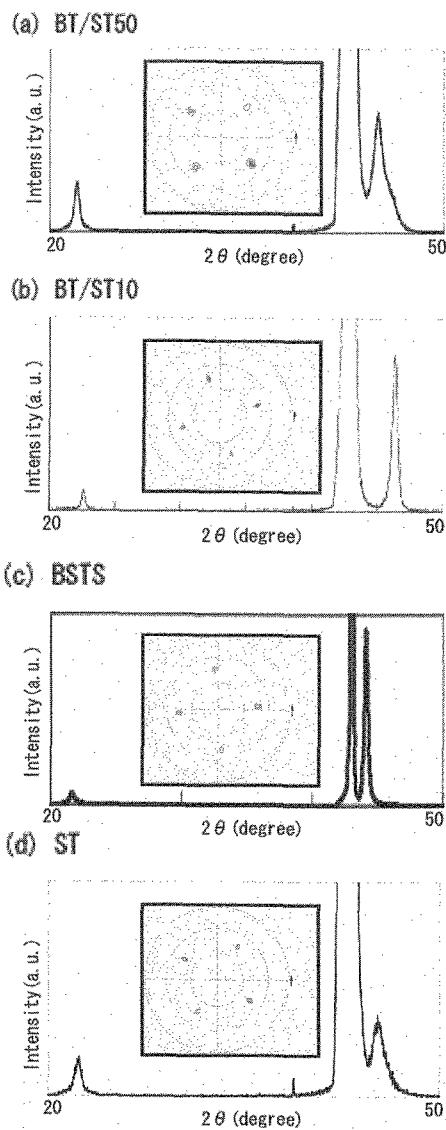


Fig. 4. XRD pattern and Pole Figure.

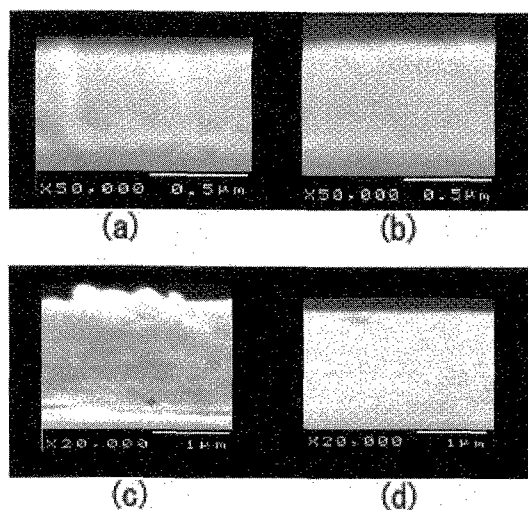


Fig. 5. Cross section SEM photograph of all samples. (a) BT/ST50, (b) BT/ST10, (c) BST, and (d) STO.

was thought that growth rate of the film on the substrate was different from deposited on the deposited film. Deposited on the substrate was slower than that of the deposited film.

We assumed that the thickness of the STO in the BT/ST50 and BT/ST10 film were half of the BT/ST50. The thickness of the each layer of each sample was shown Table III.

Table III. The thickness of each layer

sample name	thickness of film
BT/ST10	[(BTO) ₁₀ /(STO) ₁₀] ₅₀ : 250nm STO : 250nm
BT/ST50	[(BTO) ₅₀ /(STO) ₅₀] ₁₀ : 300nm STO : 250nm
BST	BST : 1350nm STO : 1350nm
STO	STO : 1700nm

3.3 Dielectric constants

Fig. 6 showed the measured results of complex admittances (Y) for the planner electrode on samples as a function of frequency in the frequency range of 1 MHz up to 3 GHz.

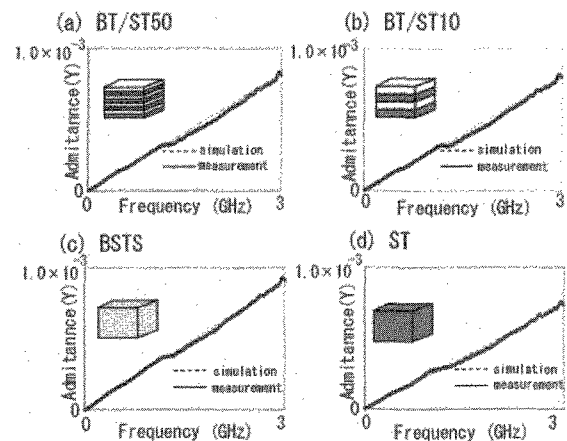


Fig. 6. Measurement results and fitting results as a function of frequency.

The BST showed the highest admittance, but multi-layered films were almost equal to BST. However, the thickness of BST was three times or more as thick as multi-layered films. So it was expected that multi-layered films showed a very high dielectric constant. The results of simulations were also indicated in Fig. 6. As a result, all films dielectric constants were shown in the following Table IV.

Table IV. Dielectric constants of each layer.

Layer	Dielectric constant
[(BTO) ₁₀ /(STO) ₁₀] ₅₀	850
[(BTO) ₅₀ /(STO) ₅₀] ₁₀	750
BST	200
STO	90

The dielectric constant of [(BTO)₁₀/(STO)₁₀]₅₀ constant of all layers. And second one was [(BTO)₁₀/(STO)₁₀]₅₀ layer which showed 750. These dielectric constants were greatly exceeded 200 of BST film that was solid solution for the

same composition. This should be due to originate in multi-layered structure. Dielectric constants of $[(\text{BTO})_n/(\text{STO})_n]_m$ artificial super lattice which made by the MBE was over 10,000. It was thought that inducing multi-layered structure, stress between the STO and BTO layer was occurred. As a result, the distortion is caused in the BTO and STO lattices, and the dielectric constant was drastically improved. The changes of the dielectric constants for the BTO/STO multi-layered film as a function of the stacking periodicities were observed from Table 10. The dielectric constant of stacking periodicity 50 was higher than that of 10. This result was conformed to the report with an artificial super-lattice. So, because of structure that looked like an artificial super lattice, multi-layered films have high dielectric constants. Prove this, the changes of the dielectric constants for the BTO/STO multi-layered film as a function of the stacking periodicities were observed from Table 10. The dielectric constant of stacking periodicity 50 was higher than that of 10. This result was conformed to the report with an artificial super-lattice.

The dielectric constant of STO and BST film was dip from theoretical figure (STO: 310, BST: over 380). In some reports, the BST and STO were fabricated more high temperature and slow growth rate of films. At low deposition temperature, crystalline is bad. And too fast growth rate, a structural defect and an empty hole were made. So to improve the dielectric constant of the films, raise deposition temperature and dropped the deposition rate.

4. Conclusion

The dielectric constant of $[(\text{BTO})_{10}/(\text{STO})_{10}]_{50}$ multi-layered film was 850. This dielectric constant was greatly exceeded BST film that was solid solution for the same composition. This result show that the possibility of fabrication BTO/STO multi-layered films like an artificial superlattice by sputtering method.

REFERENCES

- [1] T. Harigai, D. Tanaka, H. Kakemoto, S. Wada, and T. Tsurumi, *Jpn. J. Appl. Phys.* **11**, 118 (2001)
- [2] T. Tsurumi, T. Suzuki, M. Yamane, and M. Daimon, *Jpn. J. Appl. Phys.* **33**, 5192 (1994)
- [3] K. Iijima, T. Terashima, Y. Bando, K. Kamigai, and H. Terauchi, *Journal of Applied Physics*, **72**, 2840 (1992)
- [4] H. Tabata, H. Tanaka, and T. Kawaji, *Applied Physics Letters*, **65**, 1970 (1994)
- [5] O. Nakagawara, T. Shimuta, T. Makino, and S. Arai, *Applied Physics Letters*, **77**, 3257 (2000)
- [6] J. Xu, W. Menesklou, and E. Ivers-Tiffée, *Journal of the European Ceramic Society*. **24**, 1735 (2004)
- [7] I. P. Koutsaroff, T. A. Bernacki, M. Zelner, A. Cervin-Lawry, T. Jimbo, and K. Suu, *Jpn. J. Appl. Phys.* **43**, 6640 (2004)
- [8] Z. Mori, T. Nakagama, S. Higo, T. Doi, S. Koba, and Y. hakuraku, *International Journal of Modern Physics B*. **14**, 1007 (2000)
- [9] T. Tsurumi, T. Ichikawa, T. Harigai, H. Kakemoto, and S. Wada, *Journal of Applied Physics*, **91**, 2284 (2002)

(Received December 10, 2005; Accepted January 31, 2006)